

NANO EXPRESS

Open Access

Oxygen-containing functional group-facilitated CO₂ capture by carbide-derived carbons

Wei Xing^{1*}, Chao Liu¹, Ziyang Zhou², Jin Zhou², Guiqiang Wang², Shuping Zhuo², Qingzhong Xue¹, Linhua Song¹ and Zifeng Yan^{1*}

Abstract

A series of carbide-derived carbons (CDCs) with different surface oxygen contents were prepared from TiC powder by chlorination and followed by HNO₃ oxidation. The CDCs were characterized systematically by a variety of means such as Fourier transform infrared spectroscopy, X-ray photoelectron spectroscopy, ultimate analysis, energy dispersive spectroscopy, N₂ adsorption, and transmission electron microscopy. CO₂ adsorption measurements showed that the oxidation process led to an increase in CO₂ adsorption capacity of the porous carbons. Structural characterizations indicated that the adsorbability of the CDCs is not directly associated with its microporosity and specific surface area. As evidenced by elemental analysis, X-ray photoelectron spectroscopy, and energy dispersive spectroscopy, the adsorbability of the CDCs has a linear correlation with their surface oxygen content. The adsorption mechanism was studied using quantum chemical calculation. It is found that the introduction of O atoms into the carbon surface facilitates the hydrogen bonding interactions between the carbon surface and CO₂ molecules. This new finding demonstrated that not only the basic N-containing groups but also the acidic O-containing groups can enhance the CO₂ adsorbability of porous carbon, thus providing a new approach to design porous materials with superior CO₂ adsorption capacity.

Keywords: Carbide-derived carbons; CO₂ adsorption; Oxidation

Background

Observational evidence proved that global warming has already caused a series of severe environmental problems such as sea level rise, glacier melt, heat waves, wildfires, etc. [1,2]. These disasters have already greatly damaged the balance of nature. It is widely believed that the global warming in recent years is mainly ascribed to the excessive emission of greenhouse gases, in which CO₂ is the most important constituent. According to the Fourth Assessment Report which was published by Intergovernmental Panel on Climate Change (IPCC) in 2007, the annual emissions of CO₂ have grown from 21 to 38 gigatonnes (Gt) and the rate of growth of CO₂ emissions was much higher during 1995 to 2004 (0.92 Gt per year) than that of 1970 to 1994 (0.43 Gt per year) [3]. So, it is urgent to develop CO₂ capture and storage (CCS) technologies [4].

In an early stage, people used to trap CO₂ in some geological structures such as depleted oil and gas reservoirs, deep saline aquifers, unminable coal beds, etc. [5-7]. However, CO₂ geological storage usually requires large-scale equipment which calls for great costs. On the other hand, there is an obstacle to reuse the CO₂, which has been trapped in these geological structures, as an industrial raw material due to its low purity grade. So, it is necessary to develop a more feasible CCS technology.

The application of porous materials in the capture and storage of CO₂ has a big potential and wide prospect. There are many kinds of porous materials that can be used as CO₂ adsorbents, such as molecular sieves, porous silica, metal organic frameworks (MOFs), and porous carbons [8-18] due to their attractive properties such as high specific surface area and highly developed pore structure. Among these porous materials, porous carbons are especially attractive because they are inexpensive, easy to regenerate, and not sensitive to moisture which may compete with CO₂ when adsorption happens [19-21]. However, it is hard for pristine porous carbon materials

* Correspondence: xingwei@upc.edu.cn; zfyancat@upc.edu.cn

¹State Key Laboratory of Heavy Oil Processing, School of Science, China University of Petroleum, Qingdao 266580, People's Republic of China
Full list of author information is available at the end of the article

without any modification to reach high CO₂ uptake values [22]. As a result, researchers modified the surface of porous carbon with nitrogen-containing functional groups [23], which enhanced the CO₂ adsorption capacity of these porous carbon materials. For example, Chandra et al. synthesized a kind of N-doped carbon by chemical activation of polypyrrole functionalized graphene sheets. This kind of carbon material showed a CO₂ uptake of 4.3 mmol g⁻¹ with high selectivity at 298 K under 1 atm [24]. Zhou et al. prepared a series of N-doped microporous carbons using zeolite NaY as a hard template and furfuryl alcohol/acetonitrile as carbon precursors. The CO₂ adsorption capacity of as-prepared N-doped carbons was much higher than that of the template carbons without N-doping [25]. Nandi et al. prepared a series of highly porous N-doped activated carbon monoliths by physical activation. The monoliths exhibit an excellent CO₂ uptake of up to 5.14 mmol g⁻¹ at ambient temperature and 11.51 mmol g⁻¹ at 273 K under atmospheric pressure [26]. Wu et al. synthesized a series of nitrogen-enriched ordered mesoporous carbons via soft-template method. The CO₂ adsorption capacity of nitrogen-enriched carbon is higher than that of pristine material due to the presence of nitrogen-containing functionalities [27]. Sevilla et al. prepared a series of N-doped porous carbons using KOH as activation agent and polypyrrole as carbon precursor. The excellent CO₂ uptakes of these carbons were ascribed to the abundant micropores with the pore size around 1 nm and the presence of basic N-containing groups [19]. Hao et al. synthesized a kind of nitrogen-containing carbon monolith through a self-assembled polymerization of resol and benzoxazine followed by carbonization. The high CO₂ adsorption capacity was attributed to the N-containing groups of the resulting carbons [21]. The above-mentioned works all proved that the presence of nitrogen-containing functional groups can enhance the CO₂ adsorption capacities of porous carbons, and all these authors simply attribute this adsorption-enhancing effect to the acid-base interactions between acidic CO₂ molecules and basic N-containing groups without providing any experimental evidence. However, for these N-doped porous carbons that are prepared at high temperatures, the N atoms reside in the carbon skeleton and are stable at high temperatures. The basicity of these N-containing functional groups is very much weaker than that of organic amines and is rarely studied in the literatures. To the best of our knowledge, there is no direct experimental evidence to prove that this acid-base interaction does exist between CO₂ molecules and the N-containing groups of the N-doped carbon. Our previous research has proved that this CO₂ adsorption-enhancing effect for N-doped carbon is due to the hydrogen bonding interactions between CO₂ molecules and H atoms on the carbon surface. This hydrogen

bonding interactions are facilitated efficiently by N-doping, which challenges the acid-base interacting mechanism generally accepted in this field [28].

In this paper, the influence of oxygen-containing groups of the porous carbon on CO₂ capture property is studied for the first time. It is found that the presence of oxygen-containing functional groups can enhance the CO₂ adsorption capacity of porous carbons. As evidenced by both quantum chemical calculations and a variety of characterization means, this adsorption-enhancing effect is attributed to the hydrogen bond interactions between hydrogen atoms on the carbon surface and CO₂ molecules, which is greatly enhanced by the presence of O atoms on the carbon surface. As we know, most oxygen-containing functional groups such as phenolic hydroxyl groups, carboxyl groups, lactone groups, and aldehyde groups show acid tendency [29]. According to the acid-base interacting mechanism currently accepted in this field, the presence of such acidic groups would show a negative effect on CO₂ adsorption. Therefore, our work challenges the acid-base interacting mechanism currently accepted in this field. Our new finding also provides a new approach to design porous materials with superior CO₂ adsorption capacity.

Methods

Material preparation

The carbide-derived carbons (CDCs) were prepared by chlorinating TiC according to the literatures [30,31]. In the preparation, the TiC powder was placed in a quartz boat and then loaded into a quartz tube furnace. First, the quartz tube with a quartz boat inside was purged with nitrogen to thoroughly dispel oxygen. Then, the temperature of the furnace was raised to 700°C by 5°C min⁻¹ under nitrogen flow (40 mL min⁻¹). Afterwards, the nitrogen flow was shifted to chlorine flow (15 mL min⁻¹) for 3 h. The resulting powder was annealed under hydrogen at 600°C for 2 h to remove residual chlorine and chlorine-containing compounds.

To investigate the influence of oxygen content on CO₂ adsorption capacity, the as-prepared CDC was placed in a flask followed by the addition of 25 mL concentrated nitric acid for oxidation. After stirring under different temperatures for 3.5 h, the obtained carbon powder was washed thoroughly with deionized water. The dried sample was named as CDC-*x*, where *x* represents the oxidation temperature. The reduced carbon samples were obtained by heating CDC-*x* in H₂ atmosphere at 800°C for 3 h and were denoted as CDC-*x*-HR.

Material characterization

The pore structure parameters and CO₂ adsorption capacities of the carbon samples were analyzed with a surface area and porosity analyzer (ASAP 2020, Micromeritics

Corp., Norcross, GA, USA). Nitrogen sorption isotherms and CO₂ adsorption isotherms were determined at 77 and 298 K, respectively. The carbon samples were strictly degassed under vacuum (0.2 Pa) at 350°C overnight before sorption measurements. N₂ and CO₂ gases with super high purity (99.999%) were used for the sorption measurements. The specific surface area and micropore volumes of the carbons were measured by Brunauer-Emmett-Teller (BET) method and *t*-plot method, respectively. The single-point total pore volume was measured at $p/p_0 = 0.995$ and the average pore size was equal to $4V_{\text{total}}/S_{\text{BET}}$. Microscopic morphologies of the carbons were observed using a transmission electron microscope (TEM, Hitachi H800, Chiyoda, Tokyo, Japan). The chemical compositions of the carbons were determined using both a Vario EI IIIb element analyzer and an energy dispersive spectrometer (EDS; INCA Energy, Oxford, Buckinghamshire, UK). The surface chemical property of the carbons was analyzed by a X-ray photoelectron spectroscope (XPS; PHI-5000 Versaprobe, Chanhassen, MN, USA) using a monochromated Al K α excitation source. The binding energies were calibrated with respect to C1s (284.6 eV). Fourier transform infrared spectroscopy (FT-IR) analyses were carried out on a Nicolet 5800 infrared spectrometer (Madison, WI, USA) with an accuracy of 0.09 cm⁻¹. The carbons were first mixed with KBr at a mass ratio of 1/100 and then ground in an agate mortar for pressing KBr pellets.

Results and discussion

Surface properties and pore structure of carbon samples

FT-IR was used to identify oxygen-containing functional groups of the CDC samples. Compared with the pristine CDC sample before oxidation, the FT-IR spectrum of CDC-50 (Additional file 1: Figure S1) shows some new characteristic bands that were introduced by HNO₃ oxidation. The band at 3,200 to 3,600 cm⁻¹ was attributed to hydroxyl groups. The band at around 1,710 cm⁻¹ was attributed to -C=O stretching vibration. The peaks between 1,000 to 1,300 cm⁻¹ can be assigned to -C-O stretching and -OH bending modes of alcoholic, phenolic, and carboxylic groups. All this new emerging bands indicate that HNO₃ oxidation introduced a large number of oxygen-

containing functional groups, such as hydroxyl, carbonyl, and carboxyl groups, to the CDC [32-34].

Moreover, elemental analysis (EA), EDS, and XPS were employed to intensively investigate the oxygen content of the carbons. As is shown in Table 1, all these three characterization means undoubtedly demonstrate that HNO₃ oxidation did introduce a large quantity of oxygen atoms to the carbon; HNO₃ oxidation at higher temperature would introduce more oxygen atoms to the carbon; the subsequent H₂ reduction can effectively remove oxygen atoms from the oxidized carbons. For instance, as for EA data, the oxygen content of the carbons increased from 17.6 to 36.7 wt% and 41.5 wt% after oxidizing pristine CDC by HNO₃ at 50°C and 80°C, respectively. The subsequent H₂ reduction decreased the oxygen contents to 11.2 and 20.5 wt% for CDC-50 and CDC-80, respectively.

Nitrogen physisorption measurements were performed at 77 K to characterize the surface areas and pore structures of CDCs. The N₂ adsorption isotherms of all the carbons (Additional file 1: Figure S2) exhibit type I isotherms, and no hysteresis loop can be observed for these samples, indicating the microporous nature of these carbons and the absence of mesopores. The detailed specific surface area and pore structure parameters of these carbons are listed in Table 1. The specific surface area and micropore volume decrease from 1,216 m²/g and 0.59 cm³/g to 907 m²/g and 0.43 cm³/g, respectively, after oxidizing the pristine CDC by HNO₃ at 50°C, which is due to the introduction of oxygen-containing groups to the pore surface of the carbon. After H₂ reduction, the specific surface area and micropore volume increase back to 1,115 m²/g and 0.51 cm³/g, indicating that the oxygen-containing groups are effectively removed from the pore surface by H₂ reduction. This result coincides with the elemental analyses data. It is also suggested that the oxidation of the pristine CDC by HNO₃ at 50°C did not obviously damage the pore structure of the carbon and that the decrement in the specific surface area and micropore volume due to the oxidation can be mostly recovered by H₂ reduction. By contrast, oxidizing the pristine CDC by HNO₃ at 80°C results in the dramatic

Table 1 Specific surface areas, pore structure parameters, and oxygen contents of CDCs

Sample	$S_{\text{BET}}^{\text{a}}$ (m ² g ⁻¹)	$V_{\text{micro}}^{\text{b}}$ (cm ³ g ⁻¹)	$V_{\text{total}}^{\text{c}}$ (cm ³ g ⁻¹)	Pore size ^d (nm)	O content		
					EA (wt%)	XPS (wt%)	EDS (wt%)
Pristine CDC	1,216	0.59	0.65	2.13	17.6	8.7	6.8
CDC-50	907	0.43	0.47	2.06	36.7	14.6	20.3
CDC-50-HR	1,115	0.51	0.58	2.08	11.2	10.2	10.3
CDC-80	449	0.22	0.24	2.15	41.5	15.7	29.8
CDC-80-HR	497	0.22	0.27	2.21	20.5	14.2	16.0

^aBET specific surface area. ^bMicropore volumes calculated by the *t*-plot method. ^cSingle-point total pore volume measured at $p/p_0 = 0.995$. ^dPore size = $4V_{\text{total}}/S_{\text{BET}}$.

decrease of the specific surface area and micropore volume. Although the subsequent H_2 reduction can effectively remove oxygen-containing groups from CDC-80, the surface area and micropore volume cannot be recovered, indicating that HNO_3 oxidation at $80^\circ C$ severely damaged the micropore structure of the carbon.

In order to further clarify the pore structure evolution caused by HNO_3 oxidation, TEM observations were also conducted to get the microscopic morphology of the CDC. The pristine CDC (Figure 1a) shows amorphous structure and abundant micropores that are formed by the stacking of curved graphene layers. The samples CDC-50 and CDC-80 (Figure 1b,c) show similar microscopic morphology to the pristine CDC, suggesting the microporous nature of all the three samples. These results coincide with the pore size data shown in Table 1.

CO₂ capture performances of the CDCs

According to classical gas adsorption theories, gas adsorption on porous carbons usually relies on the highly developed microporous structure and large specific surface area. Recent studies also demonstrated that micropores (<1 nm) are beneficial to CO₂ adsorption for porous materials [18,35-38]. In this work, CDC-50 shows lower specific area and micropore volume (Table 1 and Figure 1d) than the pristine CDC and CDC-50-HR. However, as shown in Figure 2a, CDC-50 (3.87 mmol g^{-1} under 1 atm) possesses an apparently higher CO₂ uptake than the pristine CDC (3.66 mmol g^{-1} under 1 atm) and CDC-50-HR (2.63 mmol g^{-1} under 1 atm). Likewise, CDC-80 has a lower specific surface area and the same micropore

volume than/as its reduced product CDC-80-HR. However, the former (2.71 mmol g^{-1} under 1 atm) possesses an obviously higher CO₂ uptake than the latter (1.63 mmol g^{-1} under 1 atm). As for CDCs, their CO₂ uptakes do not have a linear correlation with their micropore volume, as is shown in Figure 2b inset. So, the CO₂ adsorption results for the CDCs cannot be explained by classical adsorption theories. Nevertheless, it is very instructive to find that the CO₂ uptakes per unit surface area of the carbons are positively related to the oxygen content of the carbons (Figure 2b), indicating that the CO₂ adsorption capacity of the carbons was greatly facilitated by the introduction of oxygen-containing groups to the carbon. This result agrees well with the work of Liu [5].

In order to reveal the effect of oxygen-containing groups on CO₂ adsorption for the carbons, a theoretical carbon surface model (OCSM) containing six different typical O-containing functional groups was developed in light of Niwa's model [39]. A pure carbon model without oxygen atoms (CSM) was also devised for comparison, as is shown in Figure 3. Density functional theory B3LYP was employed to study the interactions between these models and CO₂, and all the configurations were optimized with the 6-31 + G* basis set for all atoms using the Gaussian-03 suite package [40].

The optimized results at the 6-31 + G* level are that there are six OCSM-CO₂ complexes and six CSM-CO₂ complexes. Furthermore, the calculated results demonstrate that the frequency values of all complexes are positive, showing that they are in stable configurations. Additional file 1: Figure S3 illustrates the geometric

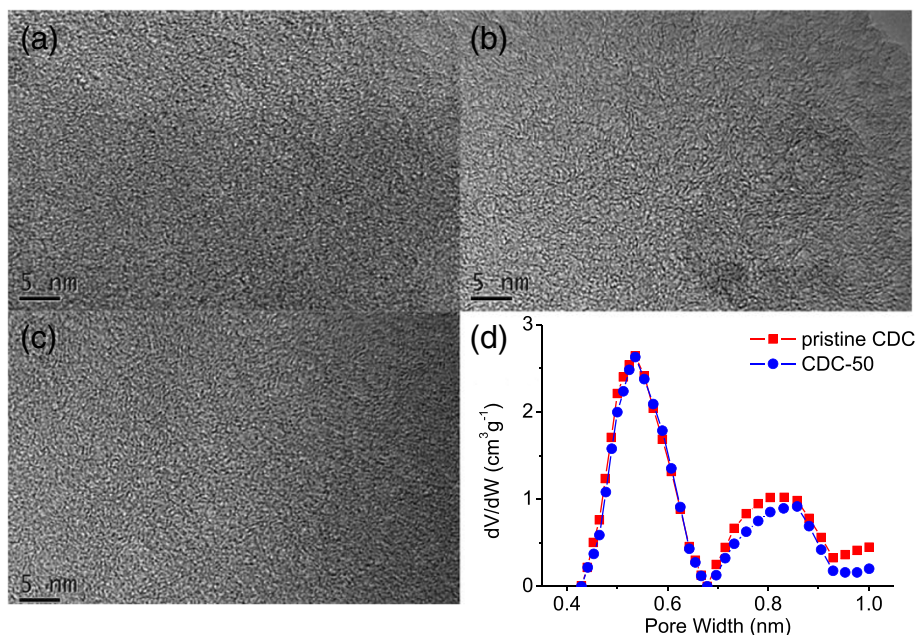


Figure 1 TEM images of CDCs: (a) CDC, (b) CDC-50, and (c) CDC-80, and (d) micropore size distribution of CDCs.

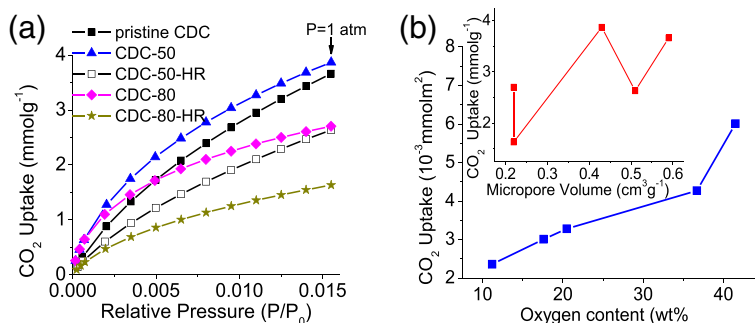


Figure 2 CO₂ adsorption isotherms for the CDCs (a) and a plot of CO₂ uptake vs. oxygen content (b). The inset is a plot of CO₂ uptake vs. micropore volume.

configurations for all the complexes, and Additional file 1: Table S1 tabulates the total energies for all the complexes. In these complexes, hydrogen bonds between CO₂ and OCSM/CSM are formed due to the high electronegativity of the oxygen atom in the CO₂ molecule. This type of weak hydrogen bond has been widely studied in recent years. The experimental and

theoretical studies have demonstrated its existence although the interaction of C-H...O is weaker than that of typical hydrogen bonds such as O-H...O and N-H...O [41-43].

Computational results indicated that the binding energies for such hydrogen bonds are different at various positions. It is apparent that the larger the bonding

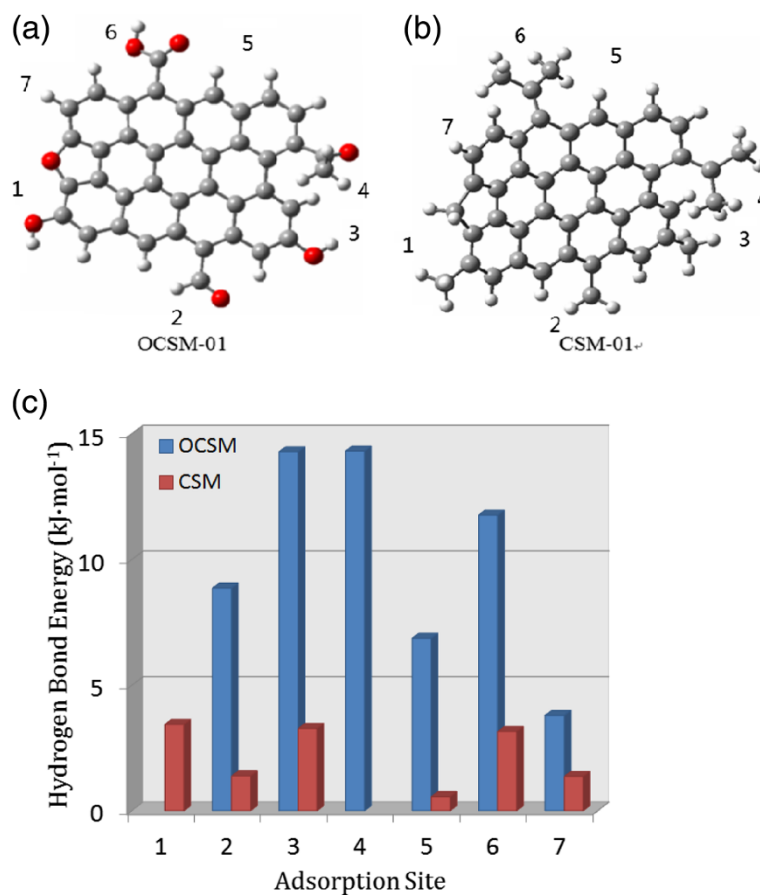


Figure 3 Theoretical carbon models and hydrogen bond energies. Theoretical models for (a) oxygen-containing carbon surface and (b) pure carbon surface (red ball: oxygen atom; grey ball: carbon atom; small grey ball: hydrogen atom). (c) Hydrogen bond energies at different adsorption sites.

energy ΔE (kJ mol^{-1}), the stronger the adsorption affinity. The average binding energy of six OCSM- CO_2 complexes is 9.98 kJ mol^{-1} , and that of CSM- CO_2 complexes is 2.20 kJ mol^{-1} , suggesting that the hydrogen bonds in the OCSM- CO_2 complexes are much stronger than those in CSM- CO_2 complexes. This binding energy difference (7.78 kJ mol^{-1}) between OCSM- CO_2 and CSM- CO_2 complexes roughly agrees with the difference of CO_2 adsorption heat between the pristine CDC and CDC-50 (as shown in Additional file 1: Figure S4), which somewhat reflects the effect of oxygen introduction on CO_2 adsorption heat for the CDCs.

In order to prove the existence of the hydrogen bonding interactions between the carbon and CO_2 molecules, FT-IR spectra (Figure 4) were recorded for CDC-50 under both N_2 and CO_2 atmospheres using a Nicolet 5700 infrared spectrometer with an accuracy of 0.1 cm^{-1} . Under N_2 atmosphere, the peak at $2,921.68 \text{ cm}^{-1}$ was attributed to the C-H anti-symmetric stretching vibration. When the atmosphere was shifted to CO_2 , this peak was broadened

and redshifted to low wavenumber, $2,919.52 \text{ cm}^{-1}$. The already published papers proved that hydrogen bonding interactions can weaken the C-H bonding energy, which lead to the redshift of corresponding peak on the FT-IR spectra [44,45]. This phenomenon confirms that the hydrogen bonding interactions between CDC-50 and CO_2 molecules do exist. Unfortunately, due to the interference caused by adsorbed water moisture on the carbon samples in FT-IR measurements, the effects of hydrogen bonding on O-H and C-O bonds cannot be observed. Besides, elemental analyses show that HNO_3 oxidation can increase the H content from 13 to 33 mmol g^{-1} for the pristine CDC and CDC-50, respectively, which enables more hydrogen bonding interactions between CDC-50 and CO_2 molecules. This also explains why the oxidized CDC samples possess higher CO_2 uptakes.

Conclusions

We intensively investigated the effect of introducing oxygen-containing functional groups to the carbon surface on the CO_2 uptake of CDCs. Structural characterizations and CO_2 adsorption on the CDCs indicate that CO_2 uptake is independent of the specific surface area and micropore volume of the CDCs but closely related to the oxygen content of the carbons. Quantum chemical calculations and FT-IR measurements reveal that the introduction of oxygen atoms into a carbon surface facilitates the hydrogen bonding interactions between the carbon surface and CO_2 molecules, which accounts for the enhanced CO_2 uptake on the oxidized CDCs. Because most oxygen-containing functional groups show acidic tendency, this new finding challenges the 'acid-base interacting mechanism' generally accepted in this field. This new finding also provides a new approach to design porous carbon with superior CO_2 adsorption capacity.

Additional file

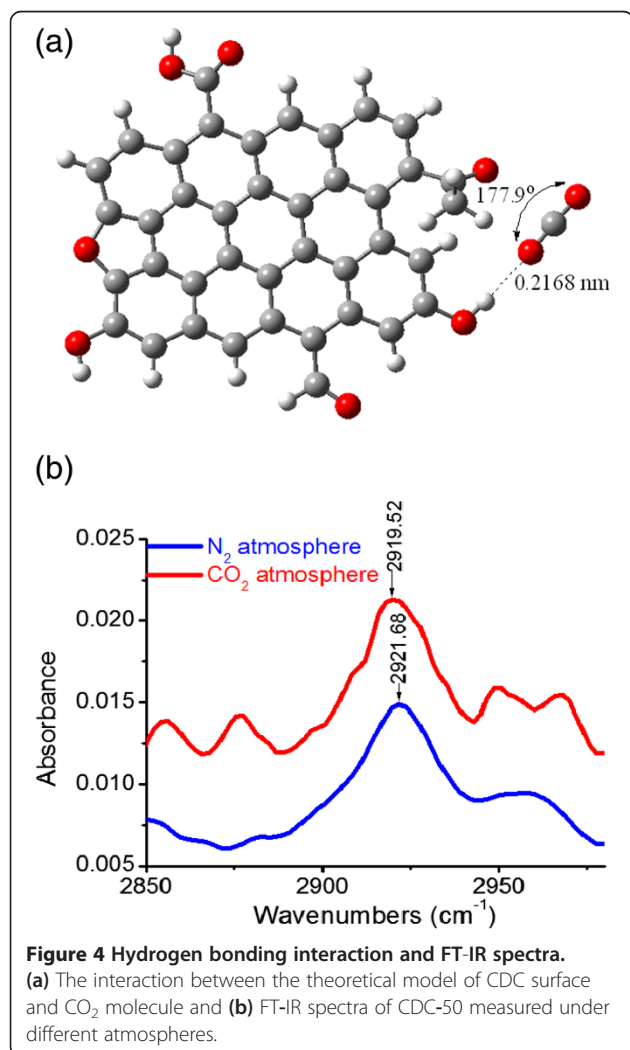
Additional file 1: Supporting information. Table S1. the total energies for OCSM- CO_2 and CSM- CO_2 complexes. Table S2. chemical composition of the CDCs determined by elemental analysis. Figure S1. FT-IR spectra of pristine CDC and CDC-50. Figure S2. nitrogen adsorption isotherms of the CDCs. Figure S3. geometric configurations and total energies for OCSM, CSM, OCSM- CO_2 complexes and CSM- CO_2 complexes. Figure S4. isosteric heats of CO_2 adsorption on the carbons at different CO_2 uptakes.

Competing interests

The authors declare that they have no competing interests.

Authors' contributions

WX and CL performed the experiments and drafted the manuscript together. ZZ performed the CO_2 adsorption simulation. JZ and GW checked the figures and gave the final approval of the version to be published. SZ, QX, and LS performed the partial experiments. ZY guided the idea and revised and finalized the manuscript. All authors read and approved the final manuscript.



Acknowledgements

This work was financially supported by the National Natural Science Foundation of China (51107076, U1362202), Distinguished Young Scientist Foundation of Shandong Province (JQ201215), Taishan Scholar Foundation (ts20130929), PetroChina Innovation Foundation (2013D-5006-0404), and China University of Petroleum (13CX02004A).

Author details

¹State Key Laboratory of Heavy Oil Processing, School of Science, China University of Petroleum, Qingdao 266580, People's Republic of China.

²School of Chemical Engineering, Shandong University of Technology, Zibo 255049, People's Republic of China.

Received: 31 March 2014 Accepted: 12 April 2014

Published: 23 April 2014

References

1. Tollefson J: Heatwaves blamed on global warming. *Nature* 2012, **488**:143–144.
2. Moritz MA: Wildfires ignite debate on global warming. *Nature* 2012, **487**:273.
3. Bernstein L, Bosch P, Canziani O, Chen Z, Christ R, Davidson O: *Climate Change 2007: Synthesis Report. An Assessment of the Intergovernmental Panel on Climate Change*. IPCC: Geneva; 2008.
4. Lund H, Mathiesen BV: The role of carbon capture and storage in a future sustainable energy system. *Energy* 2012, **44**:469–476.
5. Liu Y, Wilcox J: Effects of surface heterogeneity on the adsorption of CO₂ in microporous carbons. *Environ Sci Technol* 2012, **46**:1940–1947.
6. Chalabaud C, Robin M, Lombard JM, Martin F, Egermann P, Bertin H: Interfacial tension measurements and wettability evaluation for geological CO₂ storage. *Adv Water Resour* 2009, **32**:98–109.
7. Haszeldine RS: Carbon capture and storage: how green can black be? *Science* 2009, **325**:1647–1652.
8. Quinonero D, Frontera A, Deya PM: Feasibility of single-walled carbon nanotubes as materials for CO₂ adsorption: a DFT study. *J Phys Chem C* 2012, **116**:21083–21092.
9. Zhou H, Park J, Li J-R, Chen Y-P, Yu J, Yakovenko AA, Wang ZU, Sun LB, Balbuena PB, Zhou HC: A versatile metal-organic framework for carbon dioxide capture and cooperative catalysis. *Chem Commun* 2012, **48**:9995–9997.
10. Poloni R, Smit B, Neaton JB: CO₂ capture by metal-organic frameworks with van der Waals density functionals. *J Phys Chem A* 2012, **116**:4957–4964.
11. Sumida K, Rogow DL, Mason JA, McDonald TM, Bloch ED, Herm ZR, Bae TH, Long JR: Carbon dioxide capture in metal-organic frameworks. *Chem Rev* 2012, **112**:724–781.
12. Yi H, Deng H, Tang X, Yu Q, Zhou X, Liu H: Adsorption equilibrium and kinetics for SO₂, NO, CO₂ on zeolites FAU and LTA. *J Hazard Mater* 2012, **203**–204:111–117.
13. Yang H, Khan AM, Yuan Y, Tsang SC: Mesoporous silicon nitride for reversible CO₂ capture. *Chem Asian J* 2012, **7**:498–502.
14. Qi G, Fu L, Choi BH, Giannelis EP: Efficient CO₂ sorbents based on silica foam with ultra-large mesopores. *Energy Environ Sci* 2012, **5**:7368–7375.
15. Zheng B, Yang Z, Bai J, Li Y, Li S: High and selective CO₂ capture by two mesoporous acylamide-functionalized RHT-type metal-organic frameworks. *Chem Commun* 2012, **48**:7025–7027.
16. Yu J, Ma Y, Balbuena PB: Evaluation of the impact of H₂O, O₂, and SO₂ on postcombustion CO₂ capture in metal-organic frameworks. *Langmuir* 2012, **28**:8064–8071.
17. Wahby A, Ramos-Fernández JM, Martínez-Escandell M, Sepúlveda-Escribano A, Silvestre-Albero J, Rodríguez-Reinoso F: High-surface-area carbon molecular sieves for selective CO₂ adsorption. *ChemSusChem* 2010, **3**:974–981.
18. Jiménez V, Ramírez-Lucas A, Díaz JA, Sánchez P, Romero A: CO₂ capture in different carbon materials. *Environ Sci Technol* 2012, **6**:7407–7414.
19. Sevilla M, Valle-Vigón P, Fuertes AB: N-doped polypyrrole-based porous carbons for CO₂ capture. *Adv Funct Mater* 2011, **21**:2781–2787.
20. Drage TC, Blackman JM, Pevida C, Snape CE: Evaluation of activated carbon adsorbents for CO₂ capture in gasification. *Energy Fuel* 2009, **23**:2790–2796.
21. Hao G-P, Li W-C, Qian D, Wang G-H, Zhang W-P, Zhang T, Wang A-Q, Schüth F, Bongard H-J, Lu A-H: Structurally designed synthesis of mechanically stable poly(benzoxazine-co-resol)-based porous carbon monoliths and their application as high-performance CO₂ capture sorbents. *J Am Chem Soc* 2011, **133**:11378–11388.
22. Zhang ZQ, Wang K, Atkinson JD, Yan XL, Li X, Rood MJ, Yan Z: Sustainable and hierarchical porous *Enteromorpha prolifera* based carbon for CO₂ capture. *J Hazard Mater* 2012, **229**:183–191.
23. Gutierrez MC, Carriazo D, Ania CO, Parra JB, Ferrer ML, Del Monte F: Deep eutectic solvents as both precursors and structure directing agents in the synthesis of nitrogen doped hierarchical carbons highly suitable for CO₂ capture. *Energy Environ Sci* 2011, **4**:3535–3544.
24. Chandra V, Yu SU, Kim SH, Yoon YS, Kim DY, Kwon AH, Meyyappan M, Kim KS: Highly selective CO₂ capture on N-doped carbon produced by chemical activation of polypyrrole functionalized graphene sheets. *Chem Commun* 2012, **48**:735–737.
25. Zhou J, Li W, Zhang Z, Xing W, Zhuo S: Carbon dioxide adsorption performance of N-doped zeolite Y templated carbons. *RSC Advanc* 2012, **2**:161–167.
26. Nandi M, Okada K, Dutta A, Bhaumik A, Maruyama J, Derks D, Uyama H: Unprecedented CO₂ uptake over highly porous N-doped activated carbon monoliths prepared by physical activation. *Chem Commun* 2012, **48**:10283–10285.
27. Wu Z, Webley PA, Zhao D: Post-enrichment of nitrogen in soft-templated ordered mesoporous carbon materials for highly efficient phenol removal and CO₂ capture. *J Mater Chem* 2012, **22**:11379–11389.
28. Xing W, Liu C, Zhou ZY, Zhang L, Zhou J, Zhuo SP, Yna Z, Gao H, Wang G, Qiao SZ: Superior CO₂ uptake of N-doped activated carbon through hydrogen-bonding interaction. *Energy Environ Sci* 2012, **5**:7323–7327.
29. Maher TP, Schafer HNS: Determination of acidic functional groups in low-rank coals: comparison of ion-exchange and non-aqueous titration methods. *Fuel* 1976, **55**:138–140.
30. Presser V, McDonough J, Yeon S-H, Gogotsi Y: Effect of pore size on carbon dioxide sorption by carbide derived carbon. *Energy Environ Sci* 2011, **4**:3059–66.
31. Dash R, Chmiola J, Yushin G, Gogotsi Y, Laudisio G, Singer J, Fischer J, Kucheyev S: Titanium carbide derived nanoporous carbon for energy-related applications. *Carbon* 2006, **44**:2489–97.
32. Pradhan BK, Sandle NK: Effect of different oxidizing agent treatments on the surface properties of activated carbons. *Carbon* 1999, **37**:1323–1332.
33. Zhang Z, Xu M, Wang H, Li Z: Enhancement of CO₂ adsorption on high surface area activated carbon modified by N₂, H₂ and ammonia. *Chem Eng J* 2010, **60**:571–577.
34. Chen JP, Wu S: Acid/base-treated activated carbons: characterization of functional groups and metal adsorptive properties. *Langmuir* 2004, **20**:2233–2242.
35. Wang J, Heerwig A, Lohe MR, Oschatz M, Borchardt L, Kaskel S: Fungi-based porous carbons for CO₂ adsorption and separation. *J Mater Chem* 2012, **22**:13911–13913.
36. Martín CF, Plaza MG, Pis JJ, Rubiera F, Pevida C, Centeno TA: On the limits of CO₂ capture capacity of carbons. *Sep Purif Technol* 2010, **74**:225–229.
37. Ribeiro AM, Santos JC, Rodrigues AE, Riffart S: Pressure swing adsorption process in coal to Fischer-Tropsch fuels with CO₂ capture. *Energy Fuel* 2012, **26**:1246–1253.
38. Martín CF, Plaza MG, García S, Pis JJ, Rubiera F, Pevida C: Microporous phenol-formaldehyde resin-based adsorbents for pre-combustion CO₂ capture. *Fuel* 2011, **90**:2064–2072.
39. Niwa H, Kobayashi M, Horiba K, Harada Y, Oshima M, Terakura K: X-ray photoemission spectroscopy analysis of N-containing carbon-based cathode catalysts for polymer electrolyte fuel cells. *J Power Sources* 2011, **196**:1006–1011.
40. Frisch GWT MJ, Schlegel HB, Scuseria GE, Robb MA, Cheeseman JR, Montgomery JA Jr, Vreven T, Kudin KN, Burant JC, Millam JM, Iyengar SS, Tomasi J, Barone V, Mennucci B, Cossi M, Scalmani G, Rega N, Petersson GA, Nakatsuji H, Hada M, Ehara M, Toyota K, Fukuda R, Hasegawa J, Ishida M, Nakajima T, Honda Y, Kitao O, Nakai H, Klene M, et al: *Gaussian*. Wallingford: Gaussian, Inc; 2004.
41. Kim KH, Kim Y: Theoretical studies for lewis acid-base interactions and C–H...O weak hydrogen bonding in various CO₂ complexes. *J Phys Chem A* 2008, **112**:1596–603.

42. Matsuura H, Yoshida H, Hieda M, Yamanaka S-y, Harada T, Shin-ya K, Ohno K: **Experimental evidence for intramolecular blue-shifting C–H...O hydrogen bonding by matrix-isolation infrared spectroscopy.** *J Am Chem Soc* 2003, **125**:13910–13911.
43. Yoon S-J, Chung JW, Gierschner J, Kim KS, Choi M-G, Kim D, Park SY: **Multistimuli two-color luminescence switching via different slip-stacking of highly fluorescent molecular sheets.** *J Am Chem Soc* 2010, **132**:13675–13683.
44. Jeng MLH, DeLaat AM, Ault BS: **Infrared matrix isolation study of hydrogen bonds involving carbon-hydrogen bonds: alkynes with nitrogen bases.** *J Phys Chem* 1989, **93**:3997–4000.
45. Rozenberg M, Loewenschuss A, Marcus Y: **An empirical correlation between stretching vibration redshift and hydrogen bond length.** *Phys Chem Chem Phys* 2000, **2**:2699–2702.

doi:10.1186/1556-276X-9-189

Cite this article as: Xing et al.: Oxygen-containing functional group-facilitated CO₂ capture by carbide-derived carbons. *Nanoscale Research Letters* 2014 **9**:189.

Submit your manuscript to a SpringerOpen[®] journal and benefit from:

- ▶ Convenient online submission
- ▶ Rigorous peer review
- ▶ Immediate publication on acceptance
- ▶ Open access: articles freely available online
- ▶ High visibility within the field
- ▶ Retaining the copyright to your article

Submit your next manuscript at ▶ springeropen.com
